Journal of The Electrochemical Society, **154** (8) H743-H748 (2007)
0013-4651/2007/154(8)/H743/6/$20.00 © The Electrochemical Society

Enhancing Nanocrystallite Si Electroluminescence by Suppressing Oxygen Decomposition in High-Temperature and Low-Plasma-Power PECVD

Chun-Jung Lin[a] **and Gong-Ru Lin**[b,z]

[a]*Department of Photonics and Institute of Electro-Optical Engineering, National Chiao Tung University, Hsinchu 300, Taiwan*
[b]*Graduate Institute of Electro-Optical Engineering and Department of Electrical Engineering, National Taiwan University, Taipei 106, Taiwan*

This work demonstrates enhanced electroluminescence and quantum efficiency of a metal–SiO_x–Si light-emitting diode (MOSLED) fabricated on nanocrystallite Si (nc-Si)-embedded SiO_x plasma-enhanced chemical vapor deposition (PECVD) grown at high substrate temperature and threshold plasma power. Electron energy loss spectroscopy indicates that the energy loss of the primary electron transmitted throughout Si-rich SiO_x is reduced from 110 to 106 eV due to the formation of nc-Si. At low plasma power condition, the required dissociation energy of a N_2O molecule exceeds that of a SiH_4 molecule, while increasing the deposition temperature during PECVD growth facilitates the out-diffusion of adsorbed oxygen atoms. Such enhanced deposition of Si-rich SiO_x with excess Si atoms and dense nc-Si after annealing is observed. As the deposition temperature for the Si-rich SiO_x increases from 300 to 400°C, the electroluminescent power and quantum efficiency of the nc-Si-based MOSLED are both improved by more than 1 order of magnitude. The output power, turn-on voltage, and internal and external quantum efficiency of the indium tin oxide/SiO_x:nc-Si/p-Si/Al diode that was prepared at a substrate temperature of 400°C are 47 nW at 54 μA, 54.5 V, 5×10^{-4}, and 1.6×10^{-5}, respectively.
© 2007 The Electrochemical Society. [DOI: 10.1149/1.2747535] All rights reserved.

Manuscript submitted October 17, 2006; revised manuscript received April 17, 2007. Available electronically June 25, 2007.

Nanocrystallite Si structures that exhibit the quantum confinement effect have led to the development of novel Si-based functional devices such as light-emitting diodes, resonant tunneling diodes, and single-electron transistors, etc.[1-3] In particular, most investigations on preparing silicon oxide or nitride with buried Si nanocrystals (nc-Si) in matrices have been performed using plasma-enhanced chemical vapor deposition (PECVD), in which pure monosilane (SiH_4) and nitrous oxide (N_2O) or ammonia (NH_3) are decomposed at high plasma power from 100 to 450 W.[4,5] Few studies have addressed the deposition of Si-rich SiO_2 (SiO_x) using low-plasma-power PECVD methods. Recently, the authors demonstrated some specific features of the SiO_x thin film grown at high plasma power and low substrate temperatures for optimizing the growth of SiO_x and the precipitation of nc-Si by conventional PECVD.[6] The number of excess Si atoms in such a nonstoichiometric SiO_x matrix is increasing markedly with temperature at substrate temperatures as low as 30–100°C because of the enhanced phase separation between Si and SiO_2 during low-substrate-temperature deposition. In other words, a normal PECVD growth condition at high radio frequency (rf) power and high substrate temperature for the stoichiometric SiO_2 deposition is detrimental to the synthesis of nc-Si. However, high rf power inevitably contributes to plasma treatment on the substrate surface, which may severely worsen the electrical performance of nearby complementary metal oxide semiconductor (CMOS) devices and circuitry. A low-plasma-power PECVD synthesis of SiO_x film is therefore necessary to prevent possible damage, which was seldom discussed in previous investigations.

This work investigates the synthesis of the SiO_x film by suppressing oxygen decomposition in a low-plasma-power PECVD at high substrate temperatures. The effects of chamber pressure, SiH_4/N_2O fluence ratio, and plasma power on the excess Si ratio are characterized using continuous-wave and time-resolved photoluminescence (PL). The morphology and density of synthesized nc-Si is monitored by high-resolution transmission electron microscopy (HRTEM). In particular, the separation of Si and SiO_2 phases, the formation of nc-Si, and their transition to the crystalline phase were investigated using electron energy loss spectroscopy (EELS). The evolution of the electroluminescence (EL) of a metal-oxide-semiconductor light-emitting diode (MOSLED) that was fabricated on the PECVD-grown and nc-Si-embedded SiO_x at a high deposition temperature and threshold plasma power is also obtained.

[z] E-mail: grlin@ntu.edu.tw

Experimental

The plasma power was set as low as 40 W, and the SiO_x films were grown on p-type Si(100) substrate using a PECVD system with different SiH_4/N_2O fluence ratios, chamber pressures, and substrate temperatures. The SiH_4 fluence remained at 20 sccm, whereas the N_2O fluence varied from 105 to 130 sccm. After deposition, the samples were annealed in a quartz furnace with flowing N_2 at 1100°C for 15–180 min. The room-temperature PL of the SiO_x films, pumped by an Nd yttrium aluminum garnet (YAG) laser at a wavelength and an average intensity of 532 nm and 61 W/cm^2, respectively, was analyzed using a fluorescence spectrophotometer (CVI, DK240 with resolution of 0.06 nm) and a photomultiplier (Hamamatsu, model R928). To characterize the orientation and size of nc-Si, the bright-field cross-sectional image was taken using HRTEM (JEOL 4000EX) with a primary electron energy of 400 keV and a point-to-point resolution of 0.18 nm. In the time resolved PL (TRPL) experiment, the SiO_x samples were pumped by a third-harmonic-generated YAG laser (NY 60, Continuum) at 355 nm. The repetition rate, the pulse at the full width at half maximum (fwhm), and the average power of the YAG laser are 1 Hz, 60 ps, and 0.5 mJ/pulse, respectively. The TRPL signal was detected by a time-correlated single-photon counting system and the nc-Si-dependent luminescent lifetime was determined using Einstein's two-level quantized radiation model.[7] The PL intensity of nc-Si can be approximated by $I = \eta\sigma\phi(t)N/\tau$, where σ is the absorption cross section of nc-Si that can be determined theoretically using $\sigma = \lambda^2/8\pi\Delta\upsilon\tau$ (where λ and $\Delta\nu$ are the peak wavelength and the linewidth of the PL spectrum),[8,9] η is a relative coefficient, τ is the lifetime of nc-Si, $\phi(t)$ is the pumping flux, and N is the nc-Si concentration.[10,11]

Results and Discussion

Effect of N_2O/SiH_4 ratio on density of nc-Si in PECVD-grown SiO_x film.— Varying the N_2O/SiH_4 fluence ratio controls the Si composition in the deposited SiO_x, which strongly influences the size and density of the nc-Si after annealing. In particular, the optimal annealing condition could also be changed for the SiO_x grown at different N_2O/SiH_4 fluence ratios. Controlling SiH_4 fluence does not yield a predictable result as the decomposition rate of Si is well

Downloaded 10 Feb 2009 to 140.112.113.225. Redistribution subject to ECS license or copyright; see http://www.ecsdl.org/terms_use.jsp

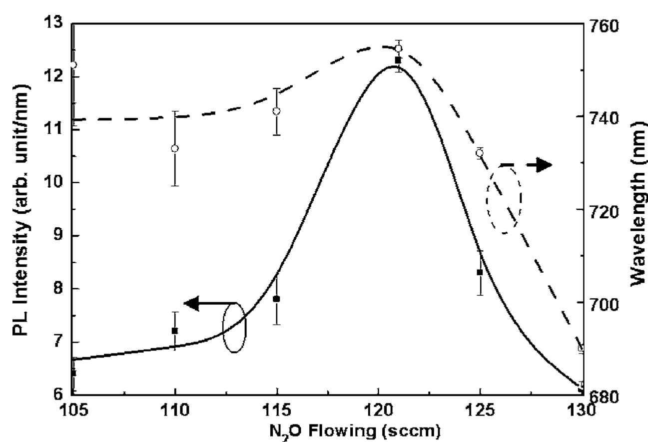

Figure 1. PL intensity and peak wavelength as a function of N_2O fluence.

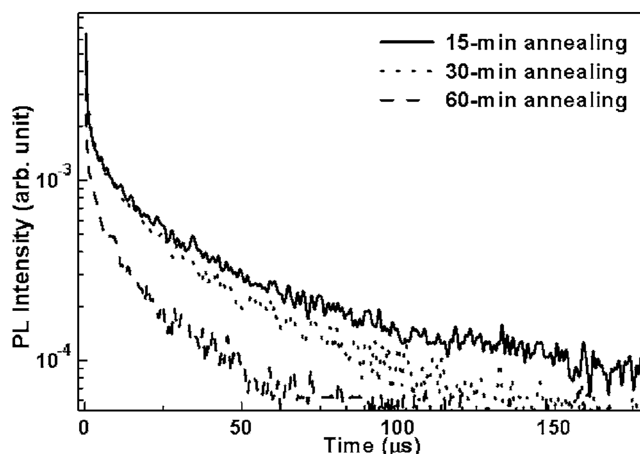

Figure 2. TRPL spectra of nc-Si embedded in PECVD-grown SiO_x samples for different annealing times.

beyond that of the oxygen under such conditions. In this case, N_2O fluence dominates the low-plasma-power PECVD growth. The optimal annealing times for SiO_x samples prepared under different N_2O fluences are tentatively varied, which is attributed to the evolutional thermal conductivity of the SiO_x caused by the variation in the density of excess Si atoms in the SiO_x film prepared under different N_2O fluences. After furnace annealing at 1100°C for 60 min, the highest PL intensity and the largest peak wavelength among these samples were observed from the sample that was prepared at an N_2O fluence of 120 sccm, as shown in Fig. 1. The highest excess Si condition was observed in the SiO_x sample that was prepared at an N_2O fluence of 120 sccm. As the N_2O fluence increased from 105 to 120 sccm, the PL intensity doubled. However, the PL intensity decreased by a factor of three as the N_2O fluence was increased further to 130 sccm. The peak PL wavelength concurrently increased from 733 to 754.5 nm as the N_2O fluence increased from 105 to 120 sccm and then decreased to 690 nm as the N_2O fluence increased to 130 sccm or higher. Increasing the N_2O fluence leads to the adsorption of more oxygen atoms on the substrate, improving oxidation and contributing to the smaller size of nc-Si, which in turn blue-shifts the PL peak after annealing. Both the size and density of nc-Si then decrease. In contrast, insufficient oxygen atoms were decomposed at N_2O fluences of under 120 sccm, yielding dense Si atoms and contributing to the larger size of nc-Si with smaller density after annealing. In addition to the observation of decreasing PL intensity, the less-decreasing trend of PL wavelength correlates closely with the almost constant size of nc-Si.

As the annealing time increases from 15 to 60 min, the lifetimes of the nc-Si in SiO_x films decrease from 52 to 20 μs, as shown in Fig. 2 and Table I. A stretched exponential function, $I(t) = I_0 \exp(-t/\tau)$, was used to fit the data, in which τ is an effective decay time. The luminescent lifetime increases from 20 to 52 μs as the nc-Si size extends from 4.0 to 4.2 nm. Moreover, the nc-Si lifetime increases smoothly with the increment of the nc-Si size, as determined by Garcia et al.[12] The theoretical carrier-transition equation can be simplified to $I_{PL} \propto \sigma\phi(t)1/\tau_{PL}N_{nc\text{-}Si}$,[12,13] and the variation of the nc-Si density can be estimated by the PL intensity (I_{PL}) and the lifetime (τ_{PL}) of nc-Si, where σ and $\phi(t)$ are the emission (absorption) cross section of nc-Si and the pumping photon flux density obtained from the pumping power, respectively. The product of these two terms for different annealing-time samples is a constant. As the annealing time increases from 15 to 60 min, the density of nc-Si decreases from 8.3 to 1.2×10^{18} cm^{-3}, which correlates closely with the evolution of measured PL, as reported by Augustine et al.[13] In principle, a longer annealing time essentially produces larger size and less-dense nc-Si because of the accumulation of small-size nc-Si and the unchanged density of Si atoms in the PECVD-grown SiO_x sample. The planar-view HRTEM image of the PECVD-grown SiO_x sample that is annealed for 15 min reveals that the average diameter of nc-Si is about 4.2 nm, as shown in Fig. 3. The fwhm of the size distribution of the nc-Si embedded in the SiO_x film is estimated to be ±1.4 nm, as shown in Fig. 4. The estimated volume density of the nc-Si buried in the 15 min annealed PECVD-grown SiO_x film is about 8.3×10^{18} cm^{-3}. In our experiment, the PL intensity of PECVD-grown SiO_x samples is the largest in the sample that is annealed for 15 min (see Fig. 5). When the annealing time gradually increases to 60 min, the excessive thermal energy

Table I. Wavelength, size, lifetime, and estimated density of nc-Si in SiO_x films after annealing for 15, 30, and 60 min.

	15 min	30 min	60 min
Wavelength (nm)	761	751	743
nc-Si size (nm)	4.2	4.1	4.0
Lifetime (μs)	52	31	20
Estimated density (cm^{-3})	8.3×10^{18}	2.4×10^{18}	1.2×10^{18}

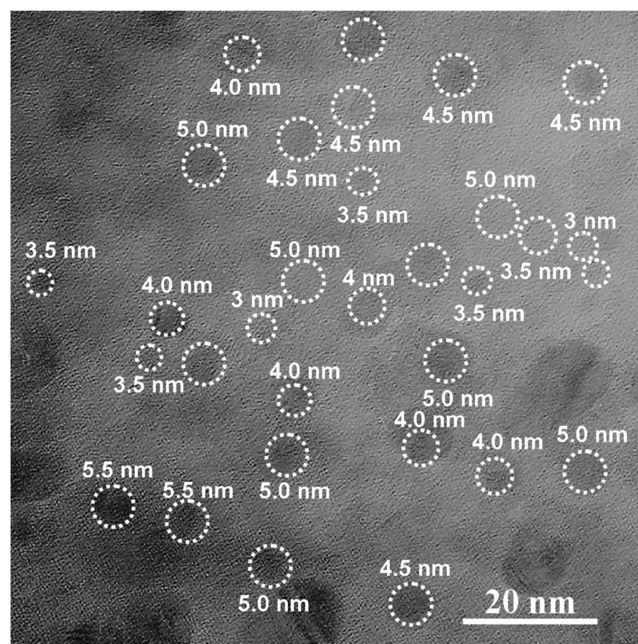

Figure 3. Planar-view HRTEM picture of 15 min annealed PECVD-grown SiO_x film.

Downloaded 10 Feb 2009 to 140.112.113.225. Redistribution subject to ECS license or copyright; see http://www.ecsdl.org/terms_use.jsp

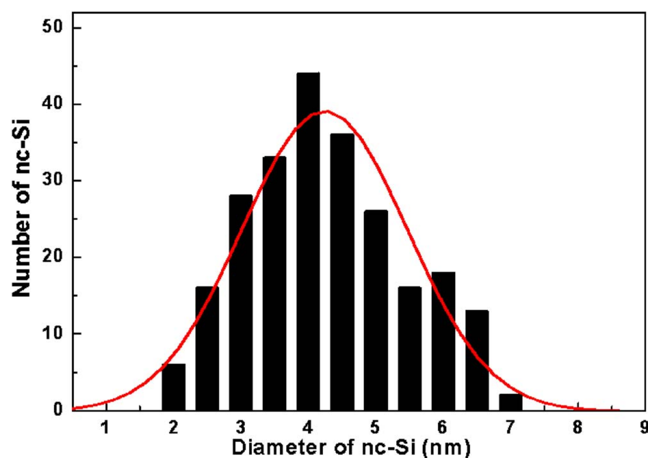

Figure 4. (Color online) Size distribution of nc-Si in the 15 min annealed PECVD-grown SiO_x film.

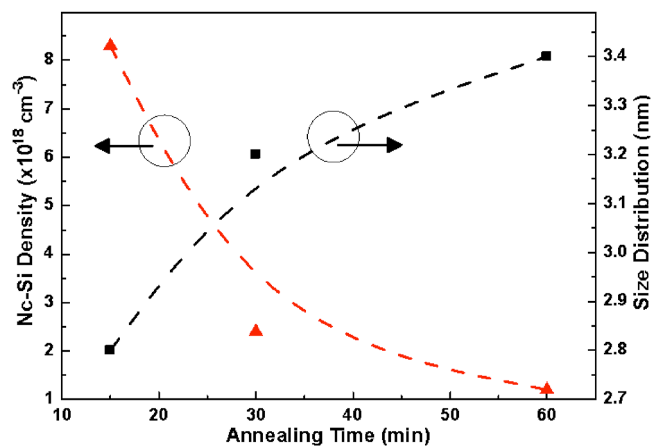

Figure 6. (Color online) Density and size distribution of nc-Si buried in annealed SiO_x film as a function of annealing time.

causes the regrowth of the SiO_2 matrix as well as the reoxidation of nc-Si. This fact can be proved by the slight blue-shift of the PL as the annealing time increases and the intensity decreases. It also is highly consistent with the result of the carrier rate equations. Indeed, the PL peak wavelengths exhibit a blue-shift from 760 to 742 nm, which correlates well with the decrease in the size of the nc-Si. Theoretically, the dominant size of nc-Si decreases from 4.5 to 4.2 nm and the width of the size distribution of nc-Si increases as annealing duration lengthens from 15 to 60 min, according to Delerue's equation[12,14] of $E(\lambda) = 1.12 + (3.73/d^{1.39})$, where $E(\lambda)$ is the wavelength-related energy and d is the size of nc-Si. Furthermore, the spectral linewidth of PL spectra $(\Delta\lambda)$ increases from 137 to 187 nm, which also corroborates the increase in the width of the size distribution (Δd) from ± 1.4 to $\pm$ 1.7 nm, as shown in Fig. 6.

The maximum PL intensities of 60 min annealed samples prepared under different chamber pressures between 40 and 70 mTorr increase with annealing time, as shown in Fig. 7. At a SiH_4/N_2O fluence ratio of 1:6, the optimal chamber pressure for the PECVD-grown SiO_x sample with the highest PL intensity is 60 mTorr, as presented in the inset of Fig. 7. The PL intensity decreases as the process pressure decreases to less than 60 mTorr. The presence of insufficient reactants at a process pressure of under 60 mTorr contributed to the lower excess Si ion density and the difficulty of precipitating nc-Si.

Effect of substrate temperature on density of nc-Si.— In EELS analysis, the primary electron that is incident the standard Si matrix with covalent Si≡Si bonds loses energy because of the versatile up-transitions of the inner shell electrons at the 2s and 2p orbits of the Si atom. Typically, $L_{2,3}$ denotes the transition of electrons at $2p_{1/2}$ and $2p_{3/2}$ orbits, and L_1 denotes that for electrons at $2s_{1/2}$ in Si. These interactions contribute to the relative peak observed at different energy losses of the EELS spectrum, in which the first peak corresponds to the up-transition of electrons from the $2p_{1/2}$ or $2p_{3/2}$ level to the vacuum. The loss of kinetic energy of the primary electron that is caused by a Si–$L_{2,3}$ transition in a standard Si substrate is about 101 eV, as shown in Fig. 8. Alternatively, the Si–$L_{2,3}$ transition in a standard SiO_2 consumes more of the energy of the primary electron, shifting the corresponding EELS peak to 110 eV with a fwhm of 4.1 eV. In the PECVD-grown SiO_x sample, the spectral linewidth is broadened to 7.7 eV as the stoichiometric condition of the SiO_x deviates from that of the SiO_2. The EELS intensity of the Si–$L_{2,3}$ transition in the PECVD-grown SiO_x sample is much lower than that of standard SiO_2 because the PECVD-grown SiO_x film is amorphous. After 30 min of furnace-annealing, the loss of the kinetic energy of the primary electron that is due to the Si–$L_{2,3}$ transition in the annealed SiO_x sample decreases to 106 eV. Moreover, the EELS intensity at a kinetic energy loss of 101 eV in the 30 min annealed sample is 2 orders of magnitude larger than that in the PECVD-grown SiO_x film, which is attributed to the formation of nc-Si. The excess Si atoms precipitate into nc-Si in the PECVD-

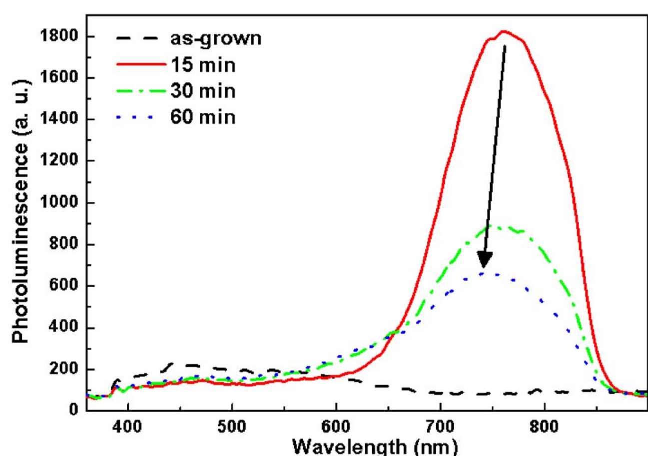

Figure 5. (Color online) PL spectra of PECVD-grown SiO_x samples annealed from 15 to 60 min.

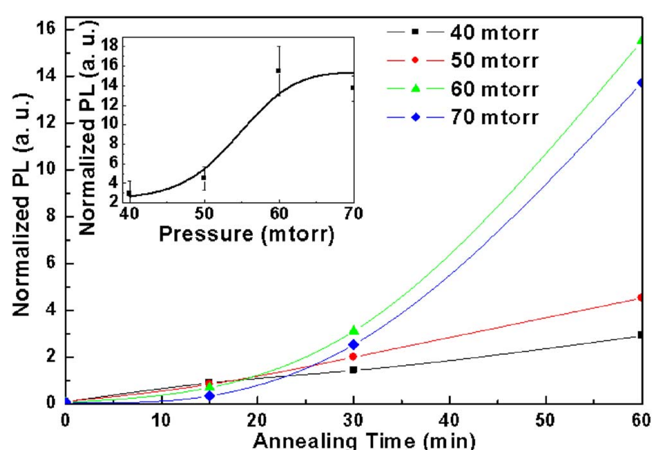

Figure 7. (Color online) PL as function of annealing time at different process pressures.

Downloaded 10 Feb 2009 to 140.112.113.225. Redistribution subject to ECS license or copyright; see http://www.ecsdl.org/terms_use.jsp

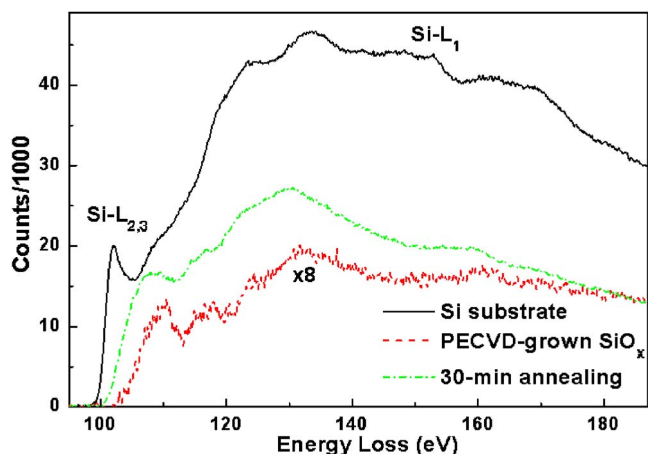

Figure 8. (Color online) EELS spectra of pure Si, as-grown SiO_x and 30 min annealed samples.

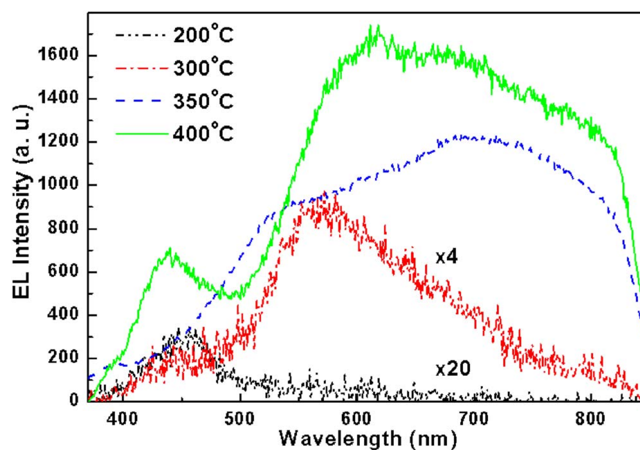

Figure 10. (Color online) EL spectra of samples prepared under different substrate temperatures.

grown SiO_x sample and the lower kinetic energy loss of a Si–$L_{2,3}$ transition in crystallite Si cause the combined kinetic energy loss of a Si–$L_{2,3}$ transition in an annealed SiO_x sample with nc-Si to be significantly lower than that in a PECVD-grown SiO_x sample without nc-Si. Therefore, the formation of nc-Si can be verified by comparing the EELS spectra of the Si substrate, the as-PECVD-grown SiO_x film, and the furnace-annealed SiO_x film, because the kinetic energy loss of a Si–$L_{2,3}$ transition varies with the chemical structure.

After furnace annealing at 1100°C for 60 min, the PL spectra of samples that are deposited at various substrate temperatures exhibit an nc-Si-dependent broad spectrum between 670 and 850 nm with a slightly broad fwhm linewidth from 101 to 106 nm as the substrate temperature increases from 200 to 400°C, as shown in Fig. 9. The PL peak wavelengths of the samples that are deposited at substrate temperatures of 200, 300, 350, and 400°C shift from 732 to 754 nm, as shown in the inset of Fig. 9, which corresponds to the increase in the size of nc-Si and the increase in the density of the excess Si atom. The normalized PL intensity of the sample deposited at a substrate temperature of 400°C is six times higher than that of the sample deposited at 200°C. At low process power (near the threshold plasma power), reactants such as SiH_4 and N_2O are hardly dissociated. Because the dissociation energies of the SiH_4 and N_2O molecules are 75.6 and 101.5 kcal/mol,[15,16] respectively, the N_2O molecule is less easily dissociated than the SiH_4 molecule, resulting in the deposition of excess Si atoms and contributing to the higher

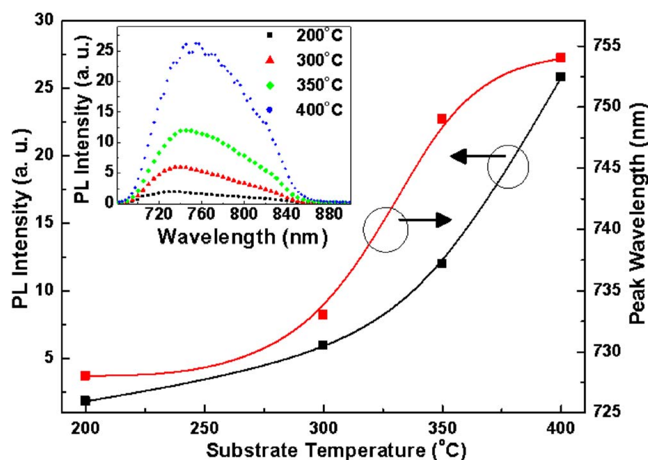

Figure 9. (Color online) PL intensity and peak wavelength as a function of substrate temperature.

density of nc-Si. Furthermore, the weight of a Si atom exceeds that of oxygen and hydrogen atoms, facilitating the deposition of Si atoms. Wong et al.[17] have also demonstrated the deposition of the carbon-doped hydrogenated silicon oxide film using PECVD at substrate temperatures from 200 to 400°C and found that the quantity of the Si-O stretching bond decreases as the deposition temperature increases, based on Fourier transform infrared spectroscopy measurements. This result is attributed to the deposition of a few oxygen atoms and the introduction of −CH and $-CH_3$ groups during the process at a high substrate temperature.

The increase of the peak intensities in the EL spectra of conventional indium tin oxide (ITO)/SiO_x:nc-Si/p-Si/Al MOSLEDs at various substrate temperatures from 200 to 400°C is well correlated with the evolution of the intensity in the PL spectra, as shown in Fig. 10. The EL intensity of the sample at a substrate temperature of 200°C is very low because the density of nc-Si is low. At lower substrate temperatures, oxygen atoms are easily adsorbed onto the substrate and hardly diffuse into free space. Therefore, the density of oxygen atoms in the PECVD-grown SiO_x film that is prepared at low substrate temperatures exceeds that of such a film prepared at a high substrate temperatures. The aforementioned reaction on the substrate contributes to the formation of a stoichiometric SiO_2 matrix. After furnace annealing at 1100°C for 60 min, sufficient oxygen atoms react with excess Si atoms to form the SiO_2 matrix. Therefore, the sample that is prepared at a substrate temperature of 200°C prefers to form a stoichiometric SiO_2 matrix and does not precipitate nc-Si, corresponding to a small EL intensity at a wavelength of 455 nm and the much-lower EL intensity at the near-infrared range. The wavelength of 455 nm is attributed to the emission of the neutral oxygen vacancy (NOV) defect. The low EL intensity at 455 nm also reveals that a few NOV defects exist in the PECVD-grown SiO_x film that is prepared at a substrate temperature of 200°C, which is like a stoichiometric SiO_2 matrix. After the substrate temperature is increased to 300°C, oxygen atoms more easily diffuse into free space than at a substrate temperature of 200°C. The density of excess Si atoms in PECVD-grown SiO_x film increases and fewer oxygen atoms react with excess Si atoms. Because the excess Si atoms are too few, little nc-Si is precipitated in the PECVD-grown SiO_x film, corresponding to the peak EL wavelength at ~600 nm. Quantum confinement effect contributes to the increase in the energy of the emission as the size of nc-Si decreases. Briefly, the luminescence at a wavelength of 455 nm for the sample that is prepared at a substrate temperature of 200°C is attributed to the emission from NOV defects; however, the luminescence at 600 nm from the sample prepared at a substrate temperature of 300°C is attributed to the emission from the small amount of nc-Si.

For the sample that is prepared at a substrate temperature of

Downloaded 10 Feb 2009 to 140.112.113.225. Redistribution subject to ECS license or copyright; see http://www.ecsdl.org/terms_use.jsp

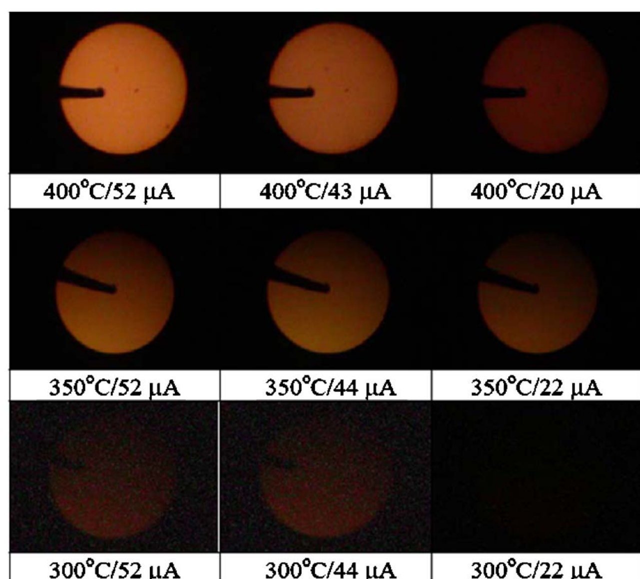

Figure 11. (Color online) Far-field patterns of ITO/SiO_x:nc-Si/p-Si/Al MOSLED.

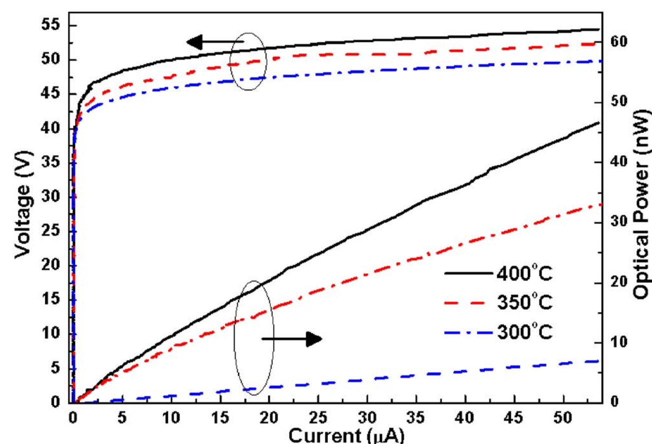

Figure 12. (Color online) *I-V* and *P-I* curves of ITO/SiO_x:nc-Si/p-Si/Al MOSLED.

350°C, EL reveals a broad spectrum between 400 and 850 nm with a peak wavelength of 700 nm and a fwhm spectral linewidth of 338 nm. The peak wavelength red-shifts from 600 to 700 nm as the temperature is increased from 300 to 350°C, revealing the increase in the size of the buried nc-Si. At a low process power and a higher substrate temperature, fewer oxygen atoms are dissociated from molecular N_2O and oxygen atoms cannot easily remain on the substrate, increasing the density of excess Si atoms in the PECVD-grown SiO_x film. The EL intensity at 700 nm of the sample prepared at a substrate temperature of 350°C is more than 1 order of magnitude higher than that of the sample prepared at 300°C, indicating an increase in the densities of nc-Si and excess Si atoms. During deposition at 350°C, oxygen atoms abruptly leave the substrate, facilitating the deposition of Si atoms. Moreover, the fwhm spectral linewidth of 338 nm for the sample prepared at 350°C is much larger than that of 140 nm for the sample prepared at 300°C, indicating that the size distribution in the 350°C sample is wider and that more excess Si atoms are embedded in the PECVD-grown SiO_x film. Increasing the substrate temperature to 400°C reduces the density of the oxygen atoms and increases the density of excess Si atoms, increasing the nc-Si density and the luminescent efficiency. The EL spectrum of the sample that is prepared at a substrate temperature of 400°C reveals a broadening linewidth from 500 to 850 nm and a peak wavelength of 618 nm with a shrunken fwhm spectral linewidth of 296 nm, which are both attributed to the emission of nc-Si. However, an EL spectrum with a peak wavelength of ~450 nm was clearly observed from PECVD-grown SiO_x film, which is attributed to the luminescence of the oxygen-related NOV defect. At the high substrate temperature, excess oxygen atoms are seldom adsorbed onto the substrate. After annealing at high temperatures, insufficient oxygen atoms can react with Si atoms and contribute to oxygen vacancies. The luminescence from NOV defects in PECVD-grown SiO_x film at high substrate temperatures reveals the deficiency of oxygen atoms during the formation of nc-Si. This result differs from that obtained for the sample that was prepared at a substrate temperature of 200°C.

At a bias current of 52 μA, ITO/SiO_x:nc-Si/p-Si/Al MOSLEDs prepared at substrate temperatures of 300, 350, and 400°C demonstrate red-color emission, which is attributed to the luminescence of nc-Si, as shown in Fig. 11. Because the density of nc-Si embedded is lowest in the sample that was prepared at a substrate temperature of 300°C, the far-field pattern of the 300°C sample demonstrates the darkest emission. The optical power is highest in the sample that was prepared at a substrate temperature of 400°C. As the substrate temperature increases, the optical power of ITO/SiO_x:nc-Si/p-Si/Al MOSLED also increases and the device becomes brighter. In other words, the high substrate temperature facilitates the out-diffusion of oxygen atoms and the increase in the number of excess Si atoms in the SiO_x film, contributing to the precipitation of nc-Si and increasing the density of nc-Si. However, unanticipated visible EL components at 455 nm associated with the oxygen vacancy defects are also observed. At a given same-bias current, the increasing EL power confirms the increase in the densities of excess Si atoms and nc-Si with the deposition temperature during PECVD growth. After annealing for 60 min, the current-voltage (*I-V*) and power-current (*P-I*) responses of the forward-biased ITO/SiO_x:nc-Si/p-Si/Al diode with the buried nc-Si are characterized, as shown in Fig. 12. The threshold voltages of the ITO/SiO_x:nc-Si/p-Si/Al prepared at 300, 350, and 400°C are 49, 46, and 44 V, respectively. A maximum output power of 47 nW, associated with a *P-I* slope of 0.84 mW/A, is obtained. According to the Fowler–Nordheim (FN) plot, a clear linear line reveals that the electron transition is the FN tunneling mechanism.[18] The *P-I* slopes of the ITO/SiO_x:nc-Si/p-Si/Al MOSLEDs are 0.84, 0.58, and 0.14 mW/A at substrate temperatures of 400, 350, and 300°C. The enlarged *P-I* slope reveals a higher density of luminescent centers, corresponding to the evolution of the PL and EL spectra. The internal quantum efficiency increases from 5.48×10^{-5} to 5×10^{-4} with a slope of 3.66×10^{-6}/ °C as the substrate temperature increases from 300 to 400°C, as plotted in Fig. 13. The external quantum efficiency increases from 2.27 $\times 10^{-6}$ to 1.6×10^{-5}. The almost linear increase in the internal quantum efficiency reveals that the density of nc-Si dominates the energy transition in ITO/SiO_x:nc-Si/p-Si/Al MOSLED, because the variation of substrate temperatures causes the density of excess Si atoms and the formation of the nc-Si.

Conclusions

The enhanced EL and external quantum efficiency of metal–SiO_x–Si MOSLEDs that are fabricated on nc-Si-embedded SiO_x PECVD-grown at high substrate temperatures and threshold plasma power are demonstrated. The formation of nc-Si and the associated structural transition were investigated using EELS. The ratio of SiH_4 and N_2O fluences, the process pressure, and the substrate temperature used in the fabrication are 1:6, 60 mTorr, and 400°C, respectively. Because the dissociation energies of the molecular SiH_4 and molecular N_2O are 75.6 and 101.5 kcal/mol, respectively, molecular N_2O dissociates less easily than molecular SiH_4, resulting in the deposition of excess Si atoms and increasing the density of nc-Si. The threshold voltages of the ITO/SiO_x:nc-Si/p-Si/Al that was pre-

Downloaded 10 Feb 2009 to 140.112.113.225. Redistribution subject to ECS license or copyright; see http://www.ecsdl.org/terms_use.jsp

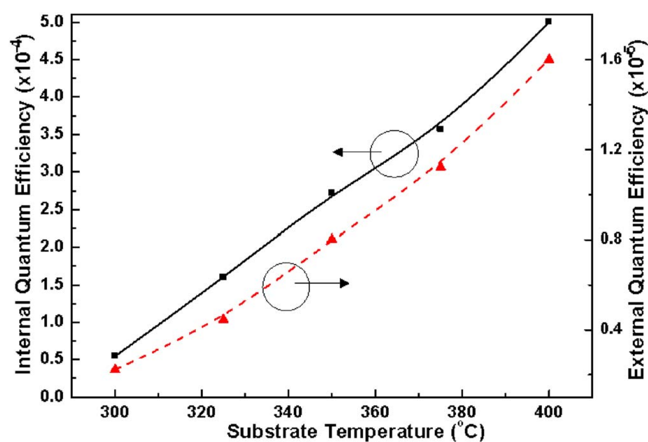

Figure 13. (Color online) Internal and external quantum efficiencies as a function of substrate temperature.

pared at 300, 350, and 400°C are 49, 46, and 44 V, respectively. The maximum output power of 47 nW, associated with a *P-I* slope of 0.84 mW/A, is determined. The internal quantum efficiency increases from 5.48×10^{-5} to 5×10^{-4} with a slope of 3.66×10^{-6}/°C. The external quantum efficiency increases from 2.27×10^{-6} to 1.6×10^{-5}.

Acknowledgments

The authors thank the National Science Council of the Republic of China, Taiwan, for financially supporting this research under contract no. NSC95-2221-E-002-448, NSC95-2120-M-009-006, NSC95-2221-E-009-282, NSC95-2752-E-229-007-PAE, and NSC96-2752-E-009-007-PAE.

National Taiwan University assisted in meeting the publication costs of this article.

References

1. G.-R. Lin, C. J. Lin, C. K. Lin, L. J. Chou, and Y. L. Chuen, *J. Appl. Phys.*, **97**, 094306 (2005).
2. M. Watanabe, T. Matsunuma, T. Maruyama, and Y. Maeda, *Jpn. J. Appl. Phys., Part 2*, **37**, L591 (1998).
3. C. H. Cho, B. H. Kim, and S. J. Park, *Appl. Phys. Lett.*, **89**, 013116 (2006).
4. G. Pucker, P. Bellutti, C. Spinella, K. Gatterer, M. Cazzanelli, and L. Pavesi, *J. Appl. Phys.*, **88**, 6044 (2000).
5. M. B. Park and N. H. Cho, *Appl. Surf. Sci.*, **190**, 151 (2002).
6. C. J. Lin, C. K. Lin, C. W. Chang, Y. L. Chueh, H. C. Kuo, Eric W. G. Diau, L. J. Chou, and G.-R. Lin, *Jpn. J. Appl. Phys., Part 1*, **45**, 1040 (2006).
7. H. Morisaki, F. W. Ping, H. Ono, and K. Yazawa, *J. Appl. Phys.*, **70**, 1869 (1991).
8. O. Madelung, *Introduction to Solid State Theory*, Chap. 6, Springer-Verlag, Berlin (1996).
9. S. Donati, *Photodetectors Devices, Circuits, and Applications*, p. 11, Prentice Hall, Englewood Cliffs, NJ (2000).
10. F. Priolo, G. Franzo, D. Pacifici, V. Vinciguerra, F. Iacona, and A. Irrera, *J. Appl. Phys.*, **89**, 264 (2001).
11. D. Kovalev, J. Diener, H. Heckler, G. Polisski, N. Kunzner, and F. Koch, *Phys. Rev. B*, **61**, 4485 (2000).
12. C. Garcia, B. Garrido, P. Pellegrino, R. Ferre, J. A. Moreno, J. R. Morante, L. Pavesi, and M. Cazzanelli, *Appl. Phys. Lett.*, **82**, 1595 (2003).
13. B. H. Augustine, E. A. Irene, Y. J. He, K. J. Price, L. E. McNeil, K. N. Christensen, and D. M. Maher, *J. Appl. Phys.*, **78**, 4020 (1995).
14. C. Delerue, G. Allan, and M. Lannoo, *Phys. Rev. B*, **48**, 11024 (1993).
15. S. H. Bauer and John A. Haberman, *IEEE J. Quantum Electron.*, **QE-14**, 233 (1978).
16. T. A. Cleland and D. W. Hess, *J. Electrochem. Soc.*, **136**, 3103 (1989).
17. T. K. S. Wong, B. Liu, B. Narayanan, V. Ligatchev, and R. Kumar, *Thin Solid Films*, **462–463**, 156 (2004).
18. M. Lenzlinger and E. H. Snow, *J. Appl. Phys.*, **40**, 278 (1969).

Downloaded 10 Feb 2009 to 140.112.113.225. Redistribution subject to ECS license or copyright; see http://www.ecsdl.org/terms_use.jsp